



## 20m Africa Rice Distribution Map of 2023

Jingling Jiang<sup>1,2,3</sup>, Hong Zhang<sup>2,1,3</sup>, Ji Ge<sup>1,2,3</sup>, Lijun Zuo<sup>1</sup>, Lu Xu<sup>1,2</sup>, Mingyang Song<sup>1,2,3</sup>, Yinhaibin Ding<sup>1,2,3</sup>, Yazhe Xie<sup>1,2,3</sup>, Wenjiang Huang<sup>1,3</sup>

<sup>1</sup>Key Laboratory of Digital Earth Science, Aerospace Information Research Institute, Chinese Academy of Sciences, Beijing 100094, China;

<sup>2</sup>International Research Center of Big Data for Sustainable Development Goals, Beijing 100049, China

<sup>3</sup>College of Resources and Environment, University of Chinese Academy of Sciences, Beijing 100049, China

Correspondence to: Hong Zhang (zhanghong@radi.ac.cn)

**Abstract.** In recent years, the demand for rice in Africa has been growing rapidly, and in order to meet this demand, the rice cultivation area is also expanding rapidly, thus it is of great significance to monitor the rice cultivation in Africa. The spatial and temporal distribution of rice cultivation in Africa is complex, making it difficult to use a climate-based rice identification method, and the existing rice distribution products are all grid based statistical data with low resolution, unable to obtain accurate rice field location and available labels. To address these two difficulties, based on time-series optical and dual-polarisation SAR data, this study proposes a sample set construction method by fast coarse positioning assisted visual interpretation, and a feature importance guided supervised classification combining multiple temporal optical and SAR features to reduce the impact of rice diversity in Africa. Firstly, we use the time-series statistical features of VH data for fast coarse positioning and screening of possible rice areas, and combine multiple auxiliary data for visual interpretation to make sample set; secondly, based on the complementary information in SAR data and optical data, the 20 meter Africa rice distribution map of 2023 was completed by combining the object-oriented segmentation results of temporal optical images and the pixel based classification results of temporal SAR data features after feature selection. The average classification accuracy of the proposed method on the validation set is more than 85%, and the  $R^2$  of the linear fit to various existing statistical data is more than 0.9, which proves that the proposed method can achieve the spatial distribution mapping of rice under the complex climatic conditions in a large region, providing crucial data support for rice monitoring and agricultural policy development. The dataset is available at <https://doi.org/10.5281/zenodo.13729353> (Jiang, Zhang et al. 2024).

### 1 Introduction

Rice is the staple food for half of the world's population (Kuenzer and Knauer 2013), providing over a quarter of the calories for approximately half of the population (Wu, Zhang et al. 2022), playing an important role in maintaining global food security and also crucial to the economies of many developing countries (Seck, Diagne et al. 2012, Ajala and Gana 2015). In 2021, rice accounted for approximately 8.3% of the world's major crop production (FAO 2023). In Africa, rice accounted for approximately 3.8% of the main crop yield and 4.7% of the global rice production. Despite its current modest



share, the demand for rice in sub-Saharan Africa is increasing at over 6% annually due to population growth, urbanization, and changes in consumer preferences, surpassing any other staple food (Arouna, Fatognon et al. 2021). In order to meet the higher demand for rice, the synchronous growth of local rice production and imports in Africa, and the expansion of rice area rather than the increase in production, are the main driving forces for the increase in domestic production. In the past thirty  
35 years, the cultivated land area has expanded by about 400,000 hectares per year (Yuan, Saito et al. 2024).

In 2023, in order to promote food and nutrition security in Africa, the African Rice Center proposed the 2030 Africa Rice Research and Innovation Strategy (AfricaRice 2023) to transform the rice based agricultural food system, and the rice area in Africa will continue to grow. Meanwhile, rice cultivation and production are important sources of income for a large number of African households (Hussain, Huang et al. 2020). However, rice cultivation in Africa also faces many challenges. Firstly,  
40 Africa is highly susceptible to the impacts of climate change, such as extreme weather events, changes in precipitation patterns, and rising temperatures, which can have a significant impact on agricultural production (Field and Barros 2014, Ogisi and Begho 2023). Land use changes across Africa, particularly urban expansion and deforestation, also influence the distribution of rice cultivation areas (Lambin and Geist 2008, Bren d'Amour, Reitsma et al. 2017). Consequently, it is essential to obtain high-resolution maps of rice spatial distribution in Africa for monitoring the condition of rice cultivation  
45 across the continent.

In recent years, the global crop mapping datasets that include rice in Africa mainly include SPAM2010 (Yu, You et al. 2020), GAEZ+2015 (Global Agro Ecological Zones) (Frolking, Wisser et al. 2020), SPAMAF2017 (International Food Policy Research 2020), and CROPGRIDS (Tang, Nguyen et al. 2023). SPAM2010 and SPAMAF2017 datasets are based on the SPAM model (Spatial Production Allocation Model) developed by the International Food Policy Research Institute (IFPRI),  
50 which utilizes geographic spatial data such as land use types and crop statistical data as inputs to make reasonable estimates of crop distribution within the decomposed units using a cross entropy approach, with a spatial resolution of 5 minute (~10km). GAEZ+2015 utilized the GAEZ model and FAO's crop statistical data to generate grid distribution products for 26 crops, with a spatial resolution of 5 minute (~10km). CROPGRIDS has generated the latest global georeferenced dataset of 173 crops using 26 published grid datasets, with a spatial resolution of 0.05° (~5.5km). The existing datasets have low  
55 resolution and are all grid maps rather than spatial distribution maps. Moreover, these data is generally outdated, making them of limited significance for monitoring rice cultivation in Africa.

Due to the complementarity of information between SAR data and optical remote sensing data, current large-scale rice mapping benefits from multi-source data that combines SAR data and optical remote sensing data as data sources (Han, Zhang et al. 2021, Shen, Pan et al. 2023, Ginting, Rudiyanto et al. 2024). Current rice mapping methods are usually divided  
60 into: 1) Phenology-based classification methods. For example, Qiu (Qiu, Li et al. 2015) utilized the CCVS (the Combined Consideration of Vegetation phenology and Surface water variations) index, constructed using LSWI and EVI during the rice heading and transplanting stages, to map rice in the complex terrain of southern China. Similarly, Zhang (Zhang, Shen et al. 2023) employed the SPRI index, which describes the growth status from the transplanting to maturity stages, to achieve



sample-free mapping of double-cropping rice. These methods do not require sample data but rely heavily on accurate phenological information. 2) Methods leveraging time-series curve similarity measures, such as DTW (Dynamic Time Warping) (Guan, Huang et al. 2016) and its improved version TWDTW (Time Weighted Dynamic Time Warping) (Singh, Rizvi et al. 2021, Tian, Li et al. 2024), requiring only a small number of rice samples to obtain a standard rice growth curve; 3) Supervised classification methods, including various machine learning methods (Wang, Zang et al. 2020, Zhang, Liu et al. 2020, You, Dong et al. 2021) and rapidly developing deep learning methods in recent years (Zhu, Zhao et al. 2021, Sun, Zhang et al. 2023). These methods offer several advantages for rice mapping. They do not require phenological information, making them adaptable to different regions and growing conditions. Additionally, they provide high classification accuracy and robustness when large amounts of labelled sample data are available. This allows for more precise identification and mapping of rice fields, even in complex landscapes or where other methods struggle. However, the effectiveness of these approaches depends on the availability and quality of the training data.

The first challenge in mapping rice in Africa lies in the significant temporal and spatial variability of rice cultivation due to its tropical and subtropical climate, as illustrated in Fig. 1. The data in this figure is derived from the rice calendar product RiceAtlas (Laborte, Gutierrez et al. 2017) published in 2017, annotating the months when the main and secondary seasons of rice planting in Africa end and harvest begins. African rice cultivation includes both single and double cropping systems, with variations in planting times and growth durations across different seasons. This makes it difficult to apply a uniform phenological description for mapping rice across the entire continent. Notably, large areas of rainfed rice cultivation (Balasubramanian, Sie et al. 2007) in Africa lack the distinct flooding signals typical of irrigated rice, which are commonly used in widely adopted rice mapping methods that rely on detecting flooding periods (Guo, Jia et al. 2019, Zhan, Zhu et al. 2021, Wei, Cui et al. 2022). Consequently, phenology-based rice mapping methods are challenging to apply in Africa. Similarly, DTW-based approaches are difficult to implement due to the variability in rice cropping intensity and phenology, which hinders the identification of a standard rice growth curve. Therefore, integrating time-series data with supervised classification emerges as the primary strategy for mapping rice spatial distribution in Africa. However, the main challenge of this approach lies in constructing sample set. Existing rice distribution products for Africa are grid-based, making it difficult to quickly identify rice-growing areas for sample set construction. Moreover, the diversity of rice cultivation in Africa—spanning phenology (including cropping intensity), farming practices (irrigated/rainfed), and environmental conditions (plains, hills)—complicates the identification of rice fields and makes it challenging to ensure the representativeness and completeness of the samples.

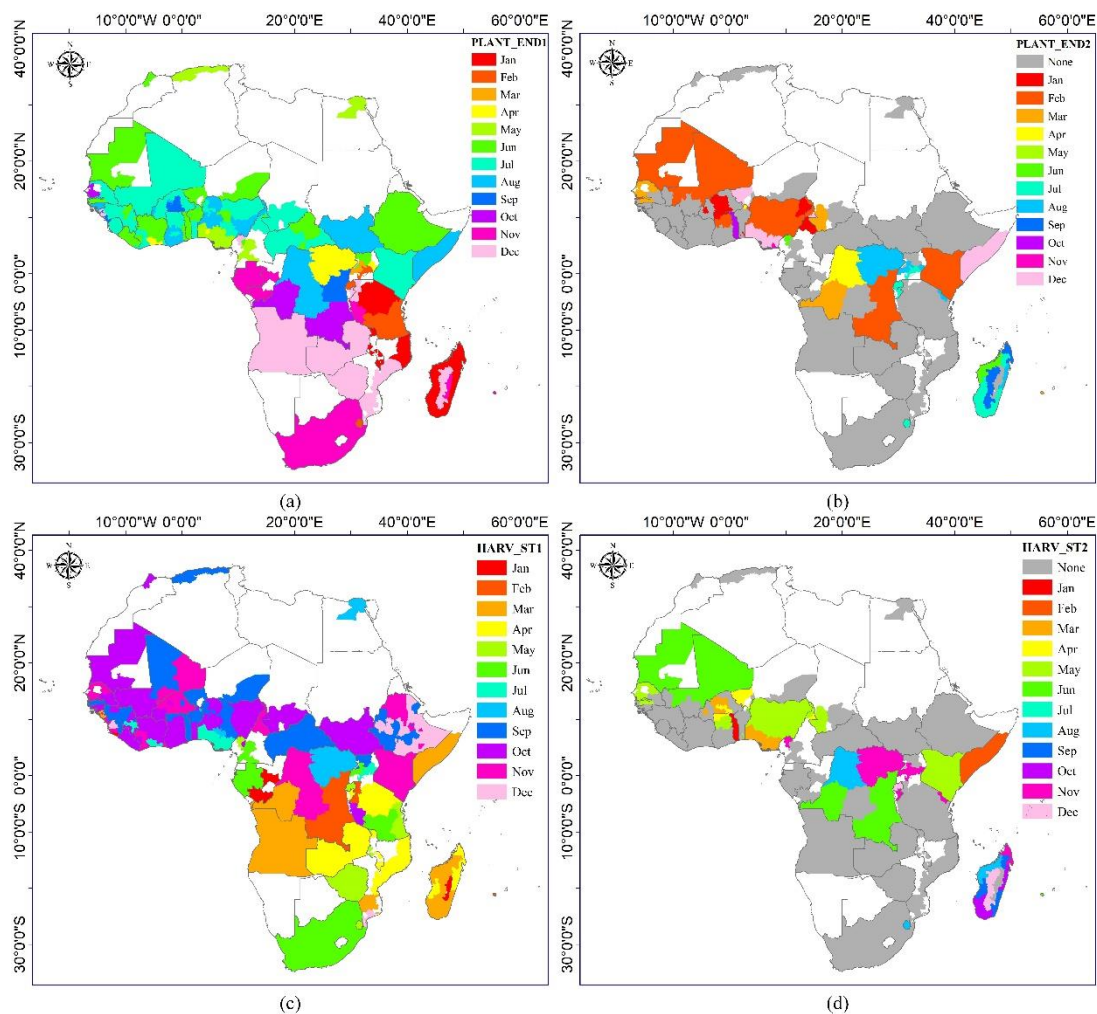


**Figure 1. Rice planting calendar: (a) main rice season planting end date, (b) secondary rice season planting end date, (c) main rice season harvest start date, and (d) secondary rice season harvest start date. Data sourced from RiceAtlas.**

95 In recent years, the Google Earth Engine (GEE) platform has provided robust support for high-resolution crop mapping. GEE integrates extensive remote sensing data and geographic information system tools, enabling rapid processing and analysis of massive time-series datasets (Gorelick, Hancher et al. 2017). In particular, Sentinel satellite data (Sentinel-1 and Sentinel-2) have been widely applied in crop monitoring and mapping due to their high spatial resolution and frequent temporal coverage (Saad El Imanni, El Harti et al. 2022, Waleed, Mubeen et al. 2022, Luo, Lu et al. 2023, Zoungrana, Barbouchi et al. 2024). Additionally, the GEE platform supports various supervised classification methods, including Random Forest (RF), Support Vector Machine (SVM), and Classification and Regression Trees (CART) (Liu, Zhai et al. 2020, You, Dong et al. 2021, Avci, Budak et al. 2023). By integrating multi-source time-series Sentinel data with these supervised classification algorithms available on the GEE platform, it has become feasible to achieve large-scale, high-resolution, and high-accuracy mapping of rice distribution in Africa.

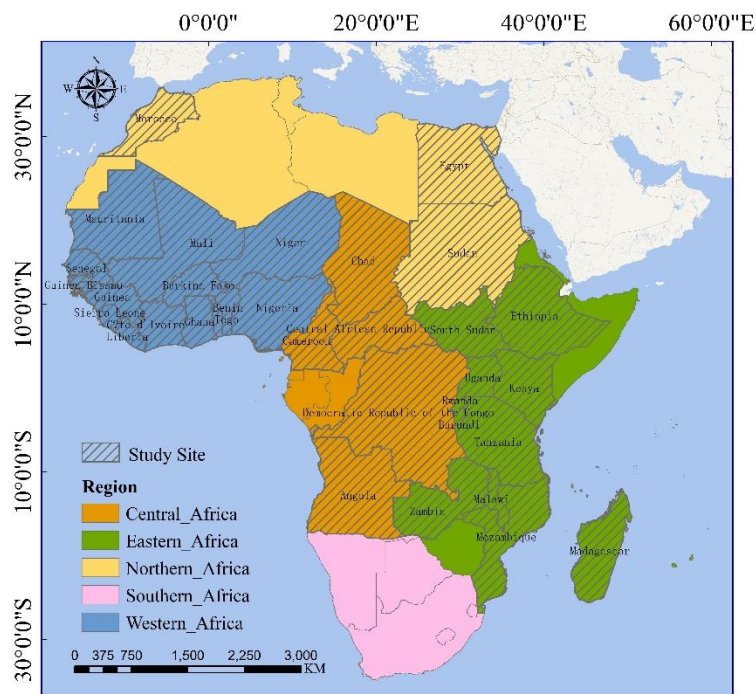


105 In summary, this study employs a multi-source time series data approach combined with classification algorithms to produce  
large scale and high-resolution rice distribution maps across in Africa. Specifically, to address the challenge of sample  
collection, time-series statistical features from Sentinel-1 VH data are used for fast coarse positioning of potential rice-  
planting areas, followed by visual interpretation using various auxiliary datasets to create reliable samples. During the  
classification stage, object-based segmentation results derived from Sentinel-2 optical time-series data are integrated with  
110 feature importance guided Random Forest classification results from Sentinel-1 SAR time-series to obtain more precise rice  
paddy boundaries and reduce noise in heterogeneous landscapes. This approach successfully generated a 20-meter resolution  
rice distribution map for Africa in 2023. The research could provide scientific support for rice management in Africa,  
contribute to improving rice yields, ensure food security, and offer data for addressing climate change. The findings are  
expected to be valuable for policymakers, agricultural scientists, and farmers alike.

## 115 **2 Materials**

### **2.1 Study site**

In this study, 34 countries with rice harvested areas exceeding 5,000 hectares, as reported by FAO statistics in 2022, were  
selected as the study regions for rice spatial distribution mapping (FAO 2022), shown in Fig. 2. These include 3 countries in  
Northern Africa (Egypt, Morocco, Sudan), 15 countries in Western Africa (Benin, Burkina Faso, Côte d'Ivoire, Gambia,  
120 Ghana, Guinea, Guinea-Bissau, Liberia, Mali, Mauritania, Niger, Nigeria, Senegal, Sierra Leone, Togo), 5 countries in  
Central Africa (Angola, Cameroon, Central African Republic, Chad, Democratic Republic of the Congo), and 11 countries in  
Eastern Africa (Burundi, Ethiopia, Kenya, Madagascar, Malawi, Mozambique, Rwanda, South Sudan, Uganda, Tanzania,  
Zambia). The regional division follows the United Nations' Geoscheme (United Nations 2013).



125 **Figure 2. Study site: 34 countries in Africa with rice harvest areas exceeding 5000 hectares in 2022 according to FAO (diagonally**  
130 **marked area)**

The climatic variations across different sub regions of Africa result in diverse rice cultivation practices. In Northern Africa, dominated by desert and Mediterranean climates, the hot and arid conditions, coupled with scarce rainfall, limit rice cultivation to areas with stable water resources, such as the Nile River basin. Rice is primarily cultivated as a single season  
130 crop, relying heavily on irrigation systems. In Western Africa, coastal regions experience tropical rainforest climates, while the interior regions have tropical savanna climates. Rainfall decreases progressively from the coast to inland, leading to rainfed rice cultivation predominantly in coastal areas during the rainy season, which typically spans from May to October, allowing for single-season planting. In inland areas, rice cultivation often depends on flood irrigation or irrigation systems, enabling multi-season cropping. Central Africa also features tropical rainforest and savanna climates, but with uneven  
135 rainfall distribution across seasons. As a result, phenological patterns of rainfed rice vary widely in rainforest areas, while rice cultivation in savanna areas partly depends on seasonal flooding or irrigation. In Eastern Africa, the highland regions are characterized by warm and humid mountain climates, where rice cultivation primarily relies on natural rainfall, with the main rainy seasons occurring from April to June and October to December. In contrast, lowland areas have tropical savanna climates, requiring irrigation support for rice cultivation.



## 140 2.2 Data source

### 2.2.1 Satellite data

The main data sources in the study are time-series SAR data and optical data. Specifically, the monthly average VH and VV data of Sentinel-1 satellite for the whole year of 2023 were obtained as SAR data input on the GEE platform, and the monthly average B3, B4, B8, and B8A band data of Sentinel-2 satellite for the whole year of 2023 were obtained as optical data input. The substantial volume of data, covering multiple spectral and temporal dimensions, enhances the model's capability to detect seasonal variations and accurately map rice fields in diverse agro-ecological zones across Africa. Table 1 presents the number of satellite images utilized for the monthly average composite across each country within the study site. A total of 29,722 Sentinel-1 (S1) images and 387,439 Sentinel-2 (S2) images were employed in the experiment.

Table 1. Number of satellite images used in the study

Num	Country	S1 image	S2 image	Num	Country	S1 image	S2 image
1	Angola	418	19765	18	Madagascar	1106	15324
2	Benin	365	2142	19	Malawi	441	3008
3	Burkina Faso	486	5126	20	Mali	1400	20949
4	Burundi	207	1126	21	Mauritania	1274	17083
5	Cameroon	1319	8253	22	Morocco	1448	8933
6	Central African Republic	963	9542	23	Mozambique	1877	26645
7	Chad	1139	19564	24	Niger	1565	18297
8	Côte d'Ivoire	514	5575	25	Nigeria	1677	14716
9	Democratic Republic of Congo	3762	55967	26	Rwanda	238	917
10	Egypt	1052	16529	27	Senegal	379	4192
11	Ethiopia	1625	17062	28	Sierra Leone	213	1872
12	Gambia	86	791	29	South Sudan	659	9882
13	Ghana	413	4407	30	Sudan	488	29213
14	Guinea	515	4704	31	Togo	120	1822
15	Guinea-Bissau	142	1233	32	Uganda	639	4534
16	Kenya	972	8917	33	United Republic of Tanzania	1427	14807
17	Liberia	245	2304	34	Zambia	548	12238

150

### 2.2.2 Land cover data

During the sample set construction phase, cropland data from the European Space Agency's ESA WorldCover data for 2020 and 2021 were used as a reference. By integrating land cover data from two consecutive years, the study ensured better



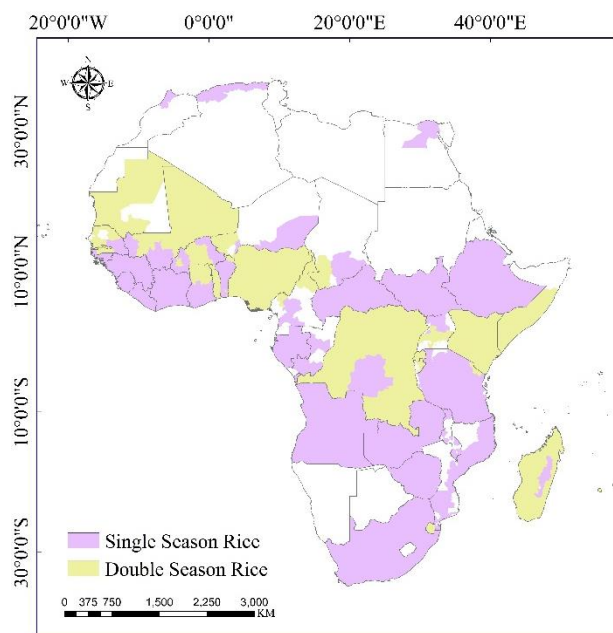
temporal consistency and reliability in sample selection. The use of this land cover data also facilitated the initial separation  
155 of rice and non-rice areas, supporting more precise training and validation in the subsequent classification processes.

### 2.2.3 Rice Grid Data

During the sample set construction phase, rice grid data from the CROPGRIDS (Tang, Nguyen et al. 2023) grid distribution  
product released in 2023 was used as a reference.

### 2.2.4 Administrative distribution data of rice planting intensity

160 In the comparison stage with statistical data, the administrative distribution data of rice planting intensity in RiceAtlas  
product (Laborte, Gutierrez et al. 2017) were used to map the rice paddy area in the mapping results to planting/harvesting  
area, and then compared with statistical data. The areas without single and double season information were defaulted to  
planting single season rice. As shown in Fig. 3.



165 **Figure 3. Administrative distribution map of rice intensity from RiceAtlas**

### 2.2.5 Statistical data

Three kinds of statistical data were used in the study, as shown in Table 2.

Table 2. Statistical data on rice area used in the study

Statistical Data	Data Time	Retrieve Time
USDA(United States Department of Agriculture):	2023	2024/02





Rice planting/harvesting area in African countries (USDA 2023)		
FAO(Food and Agriculture Organization of the United Nations): Rice harvesting area in African countries (FAO 2022)	2022	2024/03
CARD(COALITION for African Rice Development): Rice planting/harvesting area in CARD countries (CARD 2022)	2020/2021	2024/05

### 170 3 Method

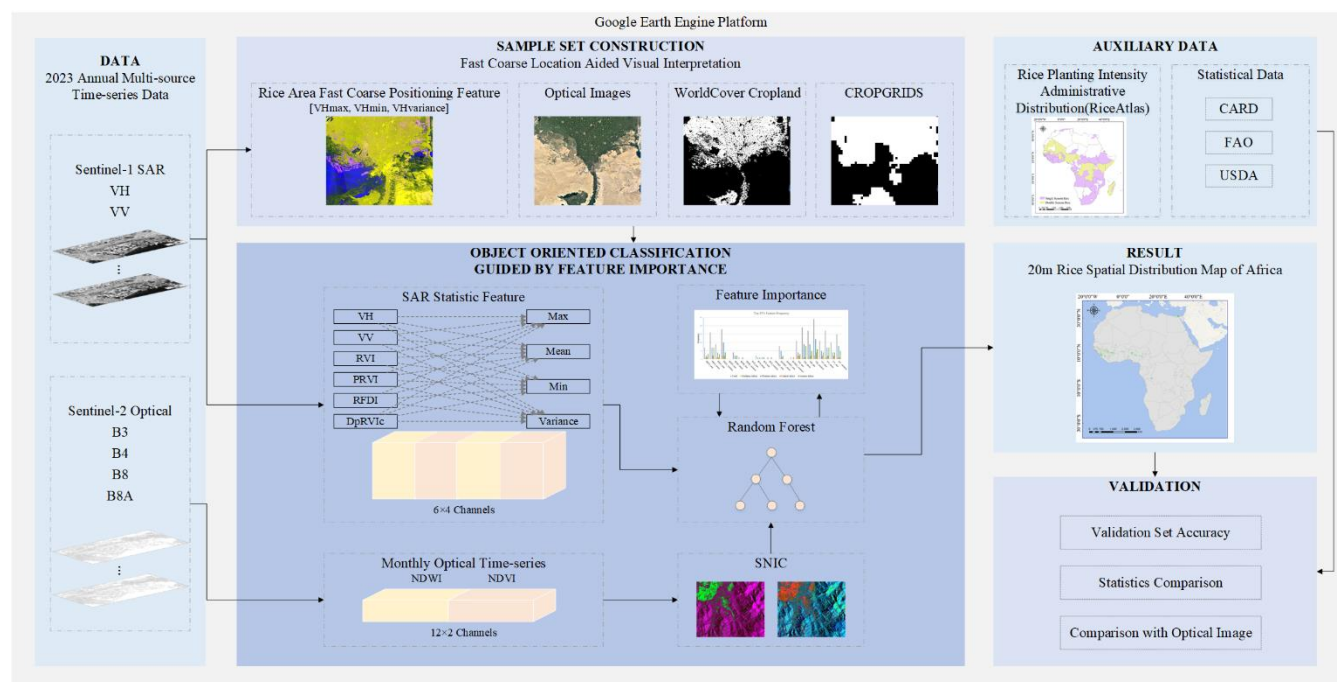


**Figure 4. Flowchart of the proposed rice mapping method (Optical images are from ©GoogleEarth)**

The workflow for mapping the spatial distribution of rice in Africa at a 20-meter resolution is depicted in Fig. 4. The study adopts a multi-source time-series data approach combined with a classifier to achieve large-scale, high-resolution mapping of rice distribution in Africa. The workflow is primarily divided into two main stages: sample set construction and object-based classification incorporating feature selection.



In the sample set construction phase, VH time-series statistical features are used for the fast coarse positioning of potential rice-growing regions. This is further refined by visually interpreting the samples using ESA WorldCover cropland data, CROPGRIDS rice grid distribution, and optical image.

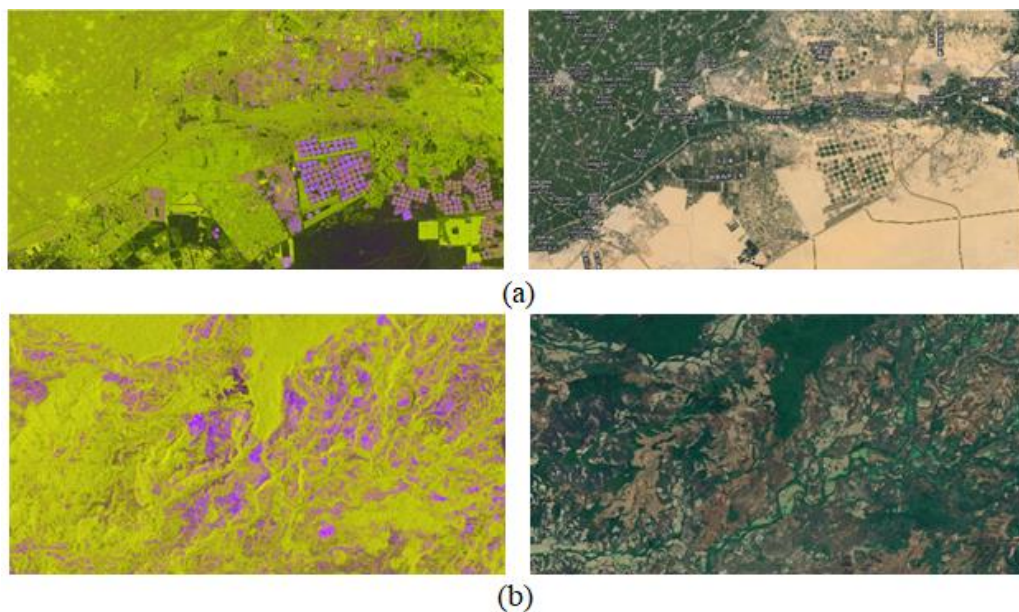
180 During the classification phase, object-based segmentation is first performed on optical images to obtain super-pixel results, which helps mitigate the effects of speckle in SAR imagery, enhances classification accuracy, and better captures the complex spatial patterns of rice fields. The mean values of SAR data (VH, VV) and various radar vegetation indices derived from SAR data within these super-pixels are then used as input features. A random forest classifier is applied to train the model, which gives ranks of the importance of the input features. The most important features are selected for a subsequent

185 classification to produce the rice paddy distribution map. Finally, accuracy validation is conducted using statistical data and validation datasets.

### 3.1 Sample set construction combined with fast coarse positioning

#### 3.1.1 Fast coarse positioning of rice planting area

Sun used the statistical features (max, min, variance) of VH time-series data for pseudo-color composite in rice mapping in Southeast Asia as input features for rice extraction (Sun, Zhang et al. 2023). In this pseudo-color feature map, rice appears purple (VHmin is small, VHmax and VHvariance are large). In the experiment, it was found that rice in Africa also exhibits similar behavior, as shown in Fig. 5. However, wetlands and other land features also exhibit similar characteristics. Therefore, it was only used for fast coarse positioning and preliminary screening of rice regions.



195 **Figure 5. Pseudo-color composite image (fast coarse positioning feature) and corresponding optical image in Africa (From ©Google Earth) (a) Plain region (b) Hilly region (R: VHmax, G: VHmin, B: VHvariance)**



### 3.1.2 Rice sample set construction

During the experiment, it was found out that wetlands and other land cover types prone to misclassification with rice also appear as purple in the pseudo-color composite image described in Section 3.1.1. Therefore, multiple auxiliary datasets were used for visual interpretation to make rice sample set. Specifically, after positioning potential rice-plating areas, rice plots were identified and selected as rice samples by cross-referencing the intersections of the rice grid map from CROPGRIDS and cropland distribution maps with corresponding optical imagery. The cropland distribution maps used the union of the cropland classes from WorldCover for the years 2020 and 2021. Additionally, in some countries, existing studies or reports, as listed in Table 3, were consulted.

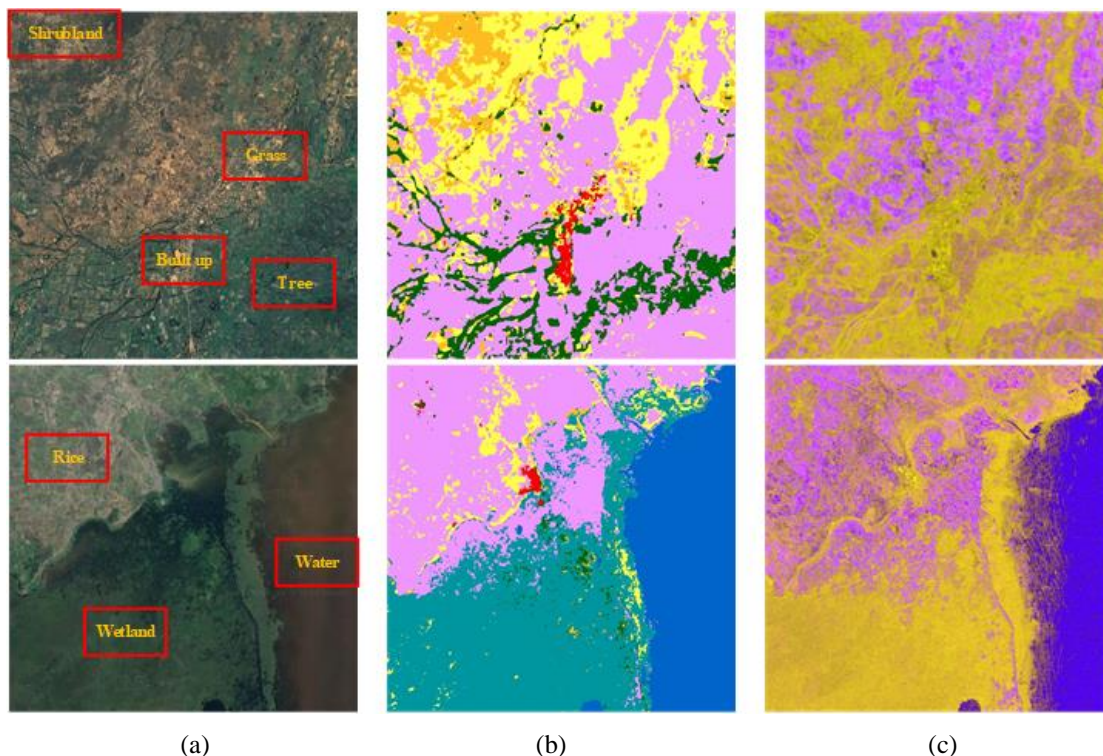
205 **Table 3. Reference for rice sample set construction in some countries**

Country	Reference
Benin	(Loko, Gbemavo et al. 2022)
Burkina Faso	(Barro, Kassankogno et al. 2021)
Egypt	(Mathieu 2022)
South Sudan	(FEWSNET 2018)

In the experiment, 50-300 rice plots were selected for each country, and 2000 rice points were randomly sampled from these plots as positive samples for the classifier input in each country's classification experiment.

### 3.1.3 Negative sample set

210 In the classification experiments conducted for each country, dozens of plots for each land cover type (non-rice cropland, built-up areas, water bodies, wetlands, forests, grasslands, etc.) were uniformly selected based on the WorldCover product. For each land cover type, 300 sample points were randomly selected as negative samples for the classifier input.



215 **Figure 6. Example of positive and negative sample regions (a) Optical image(From ©Google Earth) (b) WorldCover2021 from ESA (c) Fast coarse positioning feature**

### 3.1.4 Validation dataset

The validation dataset was constructed similarly to the training sample set. For each country, the validation dataset includes 1,000 rice sample points. Non-rice sample points were uniformly selected based on the number of land cover categories present in the WorldCover product for that country, with 100 sample points chosen for each category (with the cropland category containing only non-rice cropland samples).  
220

## 3.2 Object oriented supervised classification guided by feature importance

### 3.2.1 SNIC Object oriented segmentation

Monthly mean time-series of NDWI and NDVI data from 2023 were used as inputs to perform object-based segmentation using the Simple Non-Iterative Clustering (SNIC) algorithm (Achanta and Susstrunk 2017). This approach was adopted to  
225 reduce the fragmentation of rice paddy extraction results and enhance the clarity of rice paddy boundaries. The SNIC algorithm is a super-pixel segmentation method based on the principles of K-means clustering. It initializes seed points on a regular grid as initial cluster centers and assigns each pixel to the nearest cluster based on its distance from the cluster center in both color and spatial dimensions. Since the SNIC algorithm is non-iterative, it requires less computation time and



memory while ensuring connectivity, resulting in good segmentation performance. It is widely used in remote sensing applications (Tassi and Vizzari 2020, Wang, Meng et al. 2024).

In the experiment, the SNIC algorithm was implemented on the GEE platform with the following parameter settings: seed distance (size) = 10, segmentation compactness = 0.5, connectivity = 8, and neighbourhood size = 100.

### 3.2.2 Feature importance guided supervised classification

To address the limitations of optical imagery caused by cloud cover in large-scale mapping, SAR features were utilized after object-based segmentation based on time-series NDVI and NDWI data. The mean values of SAR features within the segmented super-pixels were used as inputs for supervised classification to achieve more accurate large-scale, high-resolution rice mapping results. This part of the study employed the Random Forest algorithm available on the GEE platform. Supervised classification experiments were first conducted for each country, with all SAR data features used as inputs to determine feature importance rankings. The top-ranked features for each region were then selected, and a second round of supervised classification was performed using these selected features to obtain the final mapping results.

The SAR features used in the experiment included VH, VV, and four commonly used radar vegetation indices: RVI (Radar Vegetation Index), PRVI (Polarimetric Radar Vegetation Index), RFDI (Radar Forest Degradation Index), and DpRVic (Dual-pol radar vegetation index for GRD data). The statistical features (max, mean, min, variance) for these indices in 2023 were utilized, as defined in Table 4.

**Table 4. Index definition**

	<b>Simplified Formula</b>
<b>RVI</b>	$\frac{4 * \sigma_{HV}}{\sigma_{VV} + \sigma_{HV}}$ (Charbonneau, Trudel et al. 2005, Li and Wang 2018)
<b>PRVI</b>	$\left(1 - \frac{\sigma_{VV}}{\sigma_{VH} + \sigma_{VV}}\right) * \sigma_{VH}$ (Chang, Shoshany et al. 2018, Sun, Zhang et al. 2024)
<b>RFDI</b>	$\frac{\sigma_{HH} - \sigma_{HV}}{\sigma_{HH} + \sigma_{HV}}$ (Chhabra, Rüdiger et al. 2022)
<b>DpRVic</b>	$q * \frac{q+3}{(q+1)^2}, q = \frac{\sigma_{HH}}{\sigma_{HV}}$ (Bhogapurapu, Dey et al. 2022)

### 3.3 Accuracy on validation set

The validation section first performs on the validation set, calculating the user accuracy (UA), producer accuracy (PA), F1-score, and overall classification accuracy (OA) for rice and non-rice categories:



250

$$UA = \frac{TP}{TP + FP} \quad (1)$$

$$PA = \frac{TP}{TP + FN} \quad (2)$$

$$F1 = 2 \times \frac{UA \times PA}{UA + PA} \quad (3)$$

$$OA = \frac{TN + TP}{TN + TP + FN + FP} \quad (4)$$

Where TP is true positive, FP is false positive, TN is true negative, and FN is false negative.

## 255 4 Results

In this section, the results and accuracy will be presented from five aspects: feature screening results, mapping and analysis of rice spatial distribution, comparison of rice area statistics results, validation set accuracy, and comparison of optical images.

### 4.1 Feature importance

260 Due to the few coverage of SAR images in Angola and Sudan, these two countries only use optical images as classification input features. In the experiments of the remaining 32 countries, a total of 24 statistical features (max, mean, min, and variance) of VH, VV, RVI, PRVI, RFDI, and DpRVic were input into random forest training to obtain feature importance ranking results. The frequency of each feature in the top 25% of feature importance ranking for each country was calculated according to the UN divided African sub region, as shown in Table 5 and Fig. 7.

265 **Table 5. Regional statistics on the frequency of features appearing in the top 25% of importance rankings (descending order)**

Total		Northern		Western		Central		Eastern	
Feature/Frequency		Feature/Frequency		Feature/Frequency		Feature/Frequency		Feature/Frequency	
VH_variance	23	PRVI_variance	2	VH_variance	24	VH_variance	4	VH_mean	8
VH_mean	18	VH_max	2	VH_mean	19	PRVI_mean	2	PRVI_mean	7
PRVI_variance	17	VH_variance	2	PRVI_variance	18	PRVI_variance	2	VV_mean	7
VH_min	17	PRVI_max	1	VH_min	17	VH_max	2	VH_variance	6
PRVI_mean	16	PRVI_min	1	VV_mean	17	VH_min	2	VH_min	5
VV_mean	16	VH_mean	1	PRVI_mean	16	VV_max	2	VV_variance	5
VV_variance	15	VH_min	1	VV_variance	15	VV_mean	2	PRVI_variance	4
VV_max	11	VV_mean	1	VH_max	11	VV_min	2	VV_max	4
VH_max	10	VV_variance	1	VV_max	11	PRVI_max	1	VV_min	4
VV_min	10	PRVI_mean	0	VV_min	10	PRVI_min	1	PRVI_max	3
PRVI_min	9	RFDI_max	0	PRVI_min	9	DpRVic_mean	1	PRVI_min	3
DpRVic_mean	8	RFDI_mean	0	DpRVic_mean	8	DpRVic_variance	1	VH_max	3
PRVI_max	6	RFDI_min	0	PRVI_max	7	VH_mean	1	RFDI_mean	2
RFDI_mean	4	RFDI_variance	0	RFDI_mean	4	VV_variance	1	DpRVic_mean	2



RVI_mean	2	RVI_max	0	RVI_mean	2	RFDI_max	0	RFDI_min	1
RFDI_min	1	RVI_mean	0	RFDI_min	1	RFDI_mean	0	RVI_mean	1
RVI_min	1	RVI_min	0	RVI_min	1	RFDI_min	0	RVI_variance	1
RVI_variance	1	RVI_variance	0	RVI_variance	1	RFDI_variance	0	RFDI_max	0
DpRVlc_variance	1	DpRVlc_max	0	DpRVlc_variance	1	RVI_max	0	RFDI_variance	0
RFDI_max	0	DpRVlc_mean	0	RFDI_max	0	RVI_mean	0	RVI_max	0
RFDI_variance	0	DpRVlc_min	0	RFDI_variance	0	RVI_min	0	RVI_min	0
RVI_max	0	DpRVlc_variance	0	RVI_max	0	RVI_variance	0	DpRVlc_max	0
DpRVlc_max	0	VV_max	0	DpRVlc_max	0	DpRVlc_max	0	DpRVlc_min	0
DpRVlc_min	0	VV_min	0	DpRVlc_min	0	DpRVlc_min	0	DpRVlc_variance	0

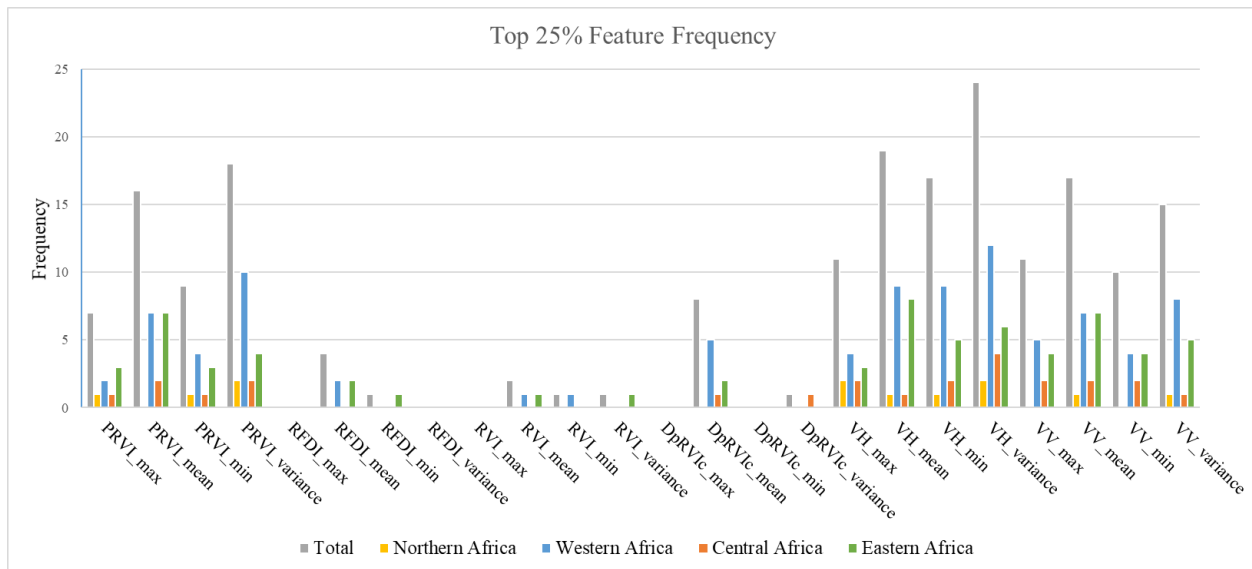
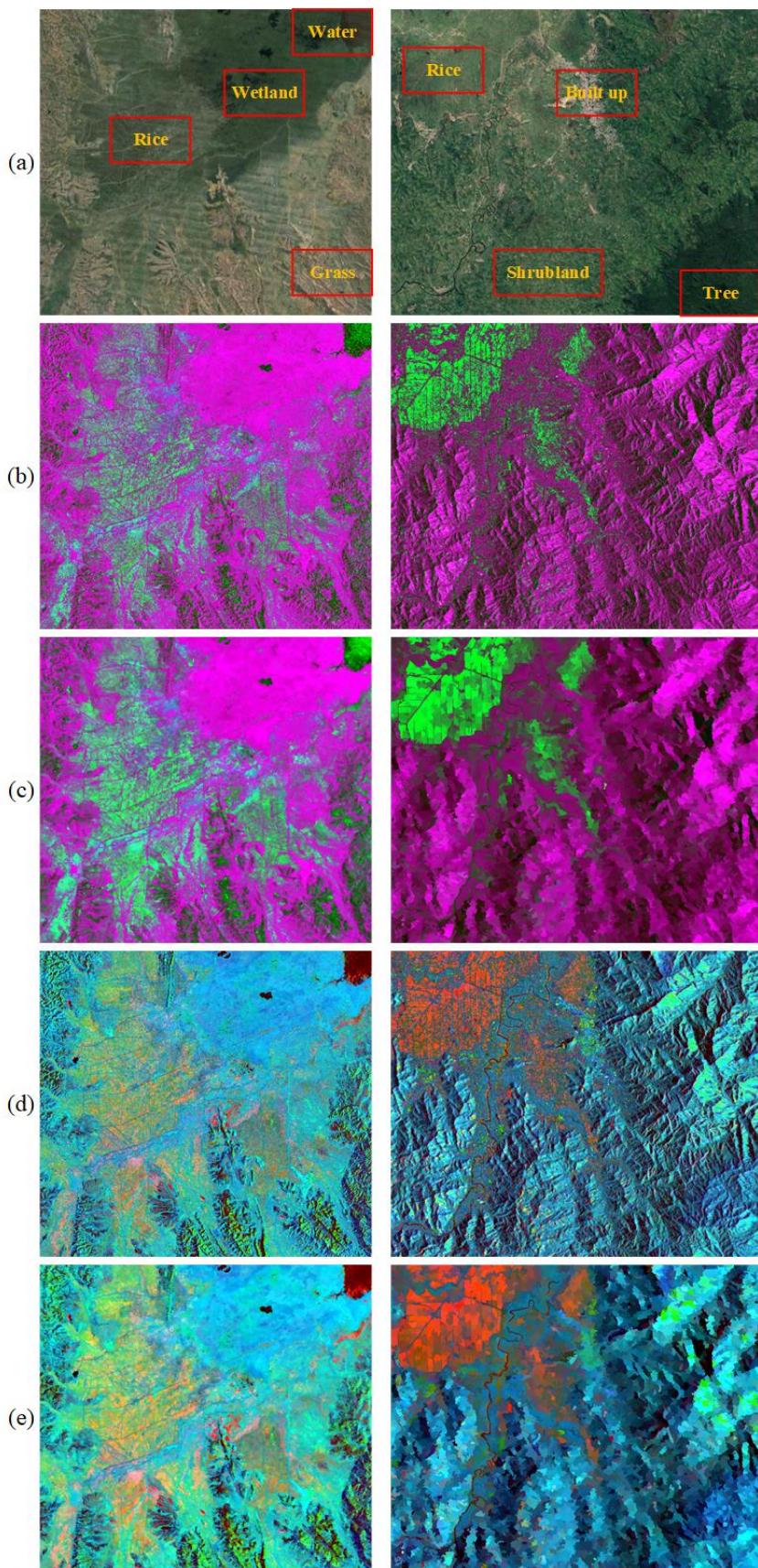


**Figure 7. Regional statistics on the frequency of features appearing in the top 25% of importance rankings (sort by feature)**

In Table 4, the features highlighted in red represent those with the highest frequency within the top 25% of importance rankings for each region (including features with tied frequencies). It can be observed that the top 25% features vary significantly across sub-regions, with the only common feature being VH\_variance. Therefore, in the Random Forest supervised classification, each sub-region used the features ranked in the top 25% in frequency for that specific sub-region. Fig. 8 illustrates an example of selected features, focusing on an area southwest of Lake Alaotra in Madagascar. The classification features used in the supervised classification for this region include six features specific to East Africa: VH\_mean, PRVI\_mean, VV\_mean, VH\_variance, VH\_min, and VV\_variance. These features were combined into two groups for pseudo-color composites, where clear distinctions between rice fields and other land cover types, including wetlands and grasslands that are prone to misclassification, can be observed. This demonstrates that the selected features effectively differentiate rice from other land cover types, enabling accurate spatial mapping of rice distribution. Additionally, the mean values calculated from object-based segmentation of optical imagery improved the representation of SAR image noise and fragmented plots while preserving clear boundaries.





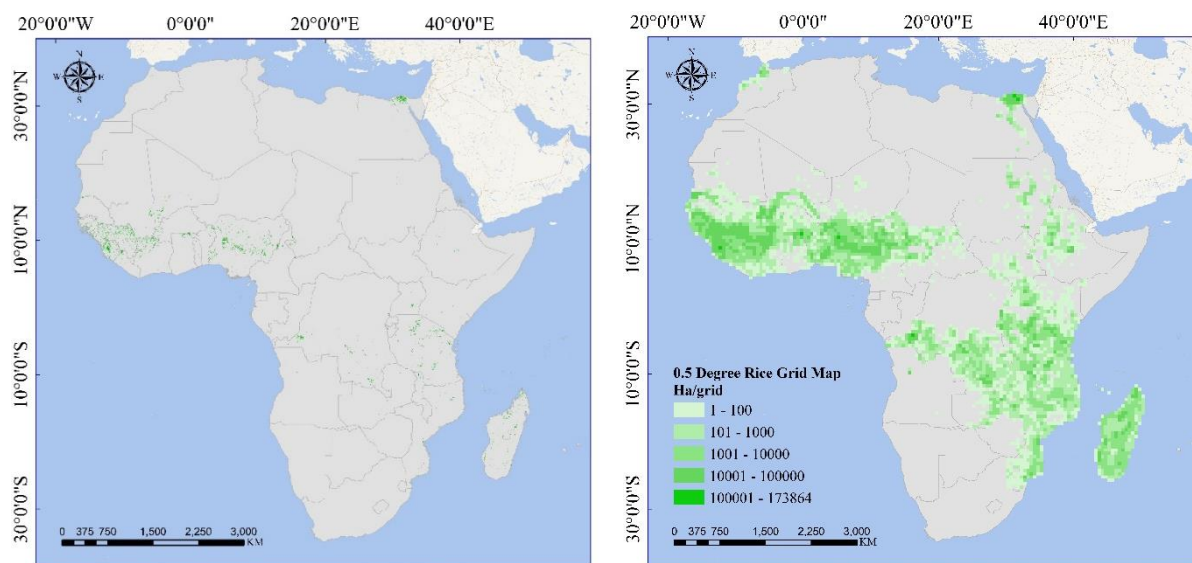


285

**Figure 8.** Example of pseudo-color composites using selected time-series SAR features: (a) optical image (From ©Google Earth) (b) pseudo-color composite 1 (R: VH\_min, G: VH\_variance, B: VH\_mean) (c) mean values of pseudo-color composite 1 overlaid on the object-based segmentation result from NDVI time series (d) pseudo-color composite 2 (R: VV\_variance, G: VV\_mean, B: PRVI\_mean); (e) mean values of pseudo-color composite 2 overlaid on the object-based segmentation result from NDVI time series.

#### 4.2 Results of rice spatial distribution mapping

Fig. 9 shows the final 20 meter resolution spatial distribution map of rice across Africa. The green areas represent rice. The map on the right displays the gridded result at a 0.5-degree resolution, with the value in the lower left corner of each grid indicating the rice area, measured in 100 hectares per grid.



290

**Figure 9.** Rice mapping result in Africa (a) 20 meter spatial distribution map (b) corresponding 0.5° grid map

**Table 6.** Country-level statistics of rice area in Africa based on the 20m spatial distribution map for 2023.

Num	Country	Paddy Area/Ha	Single Season Paddy Area/Ha	Double Season Paddy Area/Ha	Planting Area/Ha
1	Angola	30375	30375	0	30375
2	Benin	149095	82340	66755	215851
3	Burkina Faso	205356	137649	67707	273063
4	Burundi	53626	4917	48709	102335
5	Cameroon	210191	17003	193188	403379
6	Central African Republic	70545	70545	0	70545
7	Chad	283113	64938	218175	501287
8	Côte d'Ivoire	727320	727320	0	727320



9	Democratic Republic of the Congo	841988	160733	681255	1523243
10	Egypt	689114	689114	0	689114
11	Ethiopia	155157	155157	0	155157
12	Gambia	103316	0	103316	206632
13	Ghana	355311	1562	353749	709060
14	Guinea	1580359	1580359	0	1580359
15	Guinea-Bissau	178277	178277	0	178277
16	Kenya	29610	0	29610	59220
17	Liberia	135214	135214	0	135214
18	Madagascar	865405	193680	671725	1537131
19	Malawi	120866	120866	0	120866
20	Mali	502970	91772	411198	914169
21	Mauritania	63672	498	63174	126846
22	Morocco	40454	40454	0	40454
23	Mozambique	415471	415471	0	415471
24	Niger	45410	5246	40164	85573
25	Nigeria	2446413	3157	2443256	4889668
26	Rwanda	30984	0	30984	61969
27	Senegal	202077	19757	182320	384397
28	Sierra Leone	694314	694314	0	694314
29	South Sudan	48605	48605	0	48605
30	Sudan	52553	52553	0	52553
31	Togo	97076	0	97076	194153
32	Uganda	199103	29850	169253	368356
33	United Republic of Tanzania	1088377	1015933	72444	1160821
34	Zambia	83916	83916	0	83916

295 Table 6 presents the country-level statistics of rice area in Africa based on the 20m spatial distribution map for 2023. The first column represents the rice paddy area from the 2023 mapping results, the second column shows the single season rice paddy area calculated based on the rice planting intensity information from RiceAtlas, and the third column represents the double season rice field area. The fourth column provides the total planting area, with all values reported in hectares. Where

$$\text{Paddy Area} = \text{Single Season Paddy Area} + \text{Double Season Paddy Area} \quad (5)$$



$$\text{Planting Area} = \text{Single Season Paddy Area} + 2 * \text{Double Season Paddy Area} \quad (6)$$

300 The total rice paddy area across Africa in 2023 is approximately 12,795,631 hectares. Among the countries, three have rice areas exceeding 1 million hectares: Nigeria, Guinea, and Tanzania. Six countries fall within the range of 500,000 to 1 million hectares: Madagascar, the Democratic Republic of Congo (DRC), Côte d'Ivoire, Sierra Leone, Egypt, and Mali. Thirteen countries have rice areas between 100,000 and 500,000 hectares: Mozambique, Ghana, Chad, Cameroon, Burkina Faso, Senegal, Uganda, Guinea-Bissau, Ethiopia, Benin, Liberia, Malawi, and Gambia. Lastly, twelve countries have rice areas  
 305 between 50,000 and 100,000 hectares: Togo, Zambia, Central African Republic, Mauritania, Burundi, Sudan, South Sudan, Niger, Morocco, Kenya, Rwanda, and Angola. The proportion of rice area by country is illustrated in Fig. 10(a).

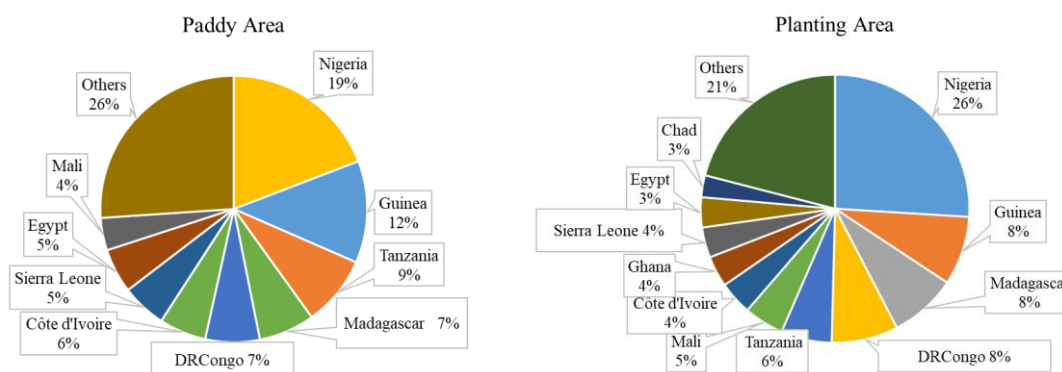


**Figure 10. Proportion of rice area by country in Africa: (a) planting area, (b) paddy area (others: aggregate of countries with areas less than 500,000 hectares).**

310 In 2023, the total rice planting/harvest area in Africa is approximately 18,739,690 hectares. Five countries have more than 1 million hectares of rice cultivation: Nigeria, Guinea, Madagascar, the Democratic Republic of the Congo (DRCongo), and Tanzania, listed in descending order by area, unless otherwise specified. Six countries have between 500,000 and 1 million hectares: Mali, Côte d'Ivoire, Ghana, Sierra Leone, Egypt, and Chad. Fourteen countries have between 100,000 and 500,000 hectares: Mozambique, Cameroon, Senegal, Uganda, Burkina Faso, Benin, Gambia, Togo, Guinea-Bissau, Ethiopia, Liberia,  
 315 Mauritania, Malawi, and Burundi. Nine countries have between 50,000 and 100,000 hectares: Niger, Zambia, Kenya, Central African Republic, Rwanda, Sudan, South Sudan, Morocco, and Angola. The proportion of rice planting area by country is shown in Fig. 10(b).

Regarding single season rice paddy, 12 countries have more than 100,000 hectares: Guinea, Tanzania, Côte d'Ivoire, Sierra Leone, Egypt, Mozambique, Madagascar, Guinea-Bissau, the Democratic Republic of the Congo, Ethiopia, Burkina Faso,  
 320 Liberia, and Malawi. For double season rice paddy, 10 countries exceed 100,000 hectares: Nigeria, the Democratic Republic of the Congo, Madagascar, Mali, Ghana, Chad, Cameroon, Senegal, Uganda, and Gambia.

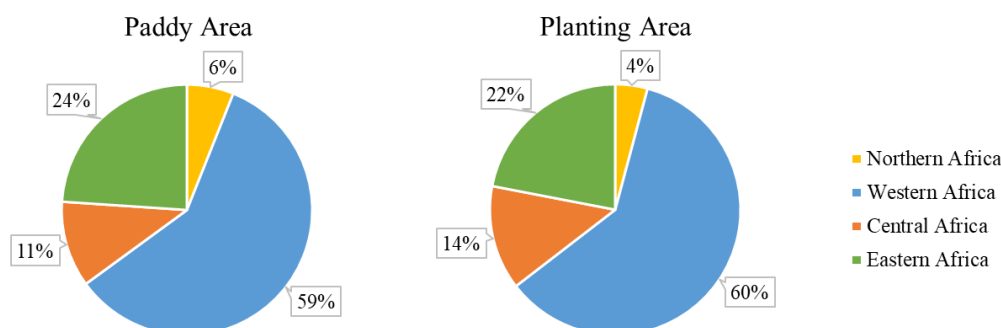


**Figure 11. Proportion of rice area by African sub-region: (a) paddy area, (b) planting area.**

Fig. 11 shows the distribution of rice area by sub-region in Africa. It can be seen that rice planting is primarily concentrated in Western Africa, followed by Eastern Africa and Central Africa, with the least in Northern Africa. Specifically, all Northern African countries plant single season rice, covering approximately 800,000 hectares, mainly in Egypt. In Western Africa, the single season rice area is around 3.7 million hectares, predominantly in Guinea, Sierra Leone, and Côte d'Ivoire, while the double season area is about 3.8 million hectares, mainly in Nigeria and Mali. In Central Africa, the single season rice area is approximately 300,000 hectares, and the double season area is about 1.1 million hectares, primarily in the Democratic Republic of the Congo. In Eastern Africa, the single season rice area is about 2.1 million hectares, mainly in Tanzania, Mozambique, and Madagascar, while the double season area is around 1 million hectares, primarily in Madagascar and Uganda. The specific distribution of major production areas is detailed in Table 7.

**Table 7. Distribution of Major Rice-Producing Regions in Africa**

Northern Africa	
Egypt	Predominantly located in the Nile Delta and the Faiyum Oasis.
Western Africa	
Nigeria	Concentrated along the western side of the Kainji Reservoir, as well as along the Niger, Benue, Sokoto, and other rivers and their tributaries.
Guinea	Mainly distributed in the coastal plains of the Boffa region in the west, the plains of the Koundara region in the northwest, and along the Niger and Sankarani rivers and their tributaries in the east.
Mali	Primarily located along the Niger River and its tributaries in the central and eastern regions.
Sierra Leone	Concentrated in the western plains.
Côte d'Ivoire	Mainly found along the Bandama River in the northwest, the Bafing region in the west, and the northern areas.
Central Africa	



Democratic Republic of the Congo  
 Predominantly located near Kinshasa and around Lake Mukamba.

---

**Eastern Africa**

Tanzania Concentrated in the Mapogoro and Itambaleo regions, the southern areas of Lake Victoria, southern Morogoro, and the Kilimanjaro region.

Madagascar Mainly distributed in the western regions of Lake Alaotra, southwestern areas, and the Ankililoaka region.

---

**4.3 Comparison of rice area and statistical data**

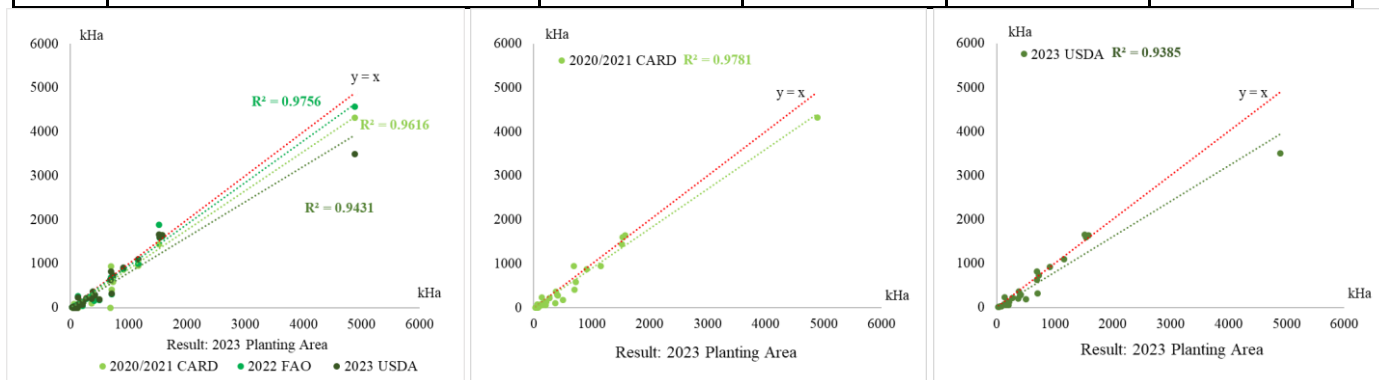
335 Table 8 presents the statistical data of rice planting areas for 34 African countries with more than 5,000 hectares of rice area, listed in alphabetical order. The first column shows the rice planting/harvest area reported by the Coalition for African Rice Development (CARD) for its member countries in 2020/2021. The second column provides the 2022 rice harvest area data from FAO. The third column shows the 2023 rice planting/harvest area reported by USDA. The fourth column presents the 2023 rice planting area derived from this study. All area units are in hectares.

340 **Table 8. Rice Area Statistics for African Countries**

Num	Country	2020/2021 CARD /Ha	2022 FAO Harvest/ Ha	2023 USDA/Ha	Planting Area/Ha
1	Angola	8572	8572	8000	30375
2	Benin	134840	134840	135000	215851
3	Burkina Faso	221052	198473	220000	273063
4	Burundi	50478	54441	0	102335
5	Cameroon	296209	156739	285000	403379
6	Central African Republic	8596	36981	/	70545
7	Chad	184086	177108	190000	501287
8	Côte d'Ivoire	581766	688201	730000	727320
9	Democratic Republic of the Congo	1442356	1888472	1660000	1523243
10	Egypt	/	646316	630000	689114
11	Ethiopia	60000	60000	60000	155157
12	Gambia	60097	46418	65000	206632
13	Ghana	414027	305000	325000	709060



14	Guinea	1650217	1627939	1650000	1580359
15	Guinea-Bissau	126654	130291	120000	178277
16	Kenya	82330	29615	30000	59220
17	Liberia	240000	257000	240000	135214
18	Madagascar	1600000	1598207	1600000	1537131
19	Malawi	76962	75787	/	120866
20	Mali	874031	888116	920000	914169
21	Mauritania	/	71000	75000	126846
22	Morocco	/	6320	8000	40454
23	Mozambique	282000	290000	290000	415471
24	Niger	12566	32414	30000	85573
25	Nigeria	4320100	4580000	3500000	4889668
26	Rwanda	31676	32253	/	61969
27	Senegal	370750	372413	370000	384397
28	Sierra Leone	944450	688549	825000	694314
29	South Sudan	/	30718	/	48605
30	Sudan	8513	10753	/	52553
31	Togo	98133	99958	94000	194153
32	Uganda	101325	260000	200000	368356
33	United Republic of Tanzania	955729	998000	1100000	1160821
34	Zambia	59601	39581	/	83916





345 **Figure 12. The linear fitting results between the 2023 rice planting area derived from this study and the existing statistical data, with mapping results as the x-axis and existing statistical data as the y-axis. The red dashed line represents the  $y = x$  line. (a) fitting results for all 34 countries, (b) fitting results for 30 countries after excluding those with missing data from the CARD dataset (c) fitting results for 27 countries after excluding those with missing data from the USDA dataset.**

The comparison between the calculated rice planting areas from mapping result and the rice intensity distribution data, alongside existing statistical data, reveals strong linear relationship, as shown in Fig. 12. For all 34 countries, the  $R^2$  value for fitting with CARD data (2020/2021) is 0.9616, with FAO data (2022) is 0.9756, and with USDA data (2023) is 0.9431. After  
350 data (27 countries) it is 0.9385, demonstrating strong consistency.

The figures and tables indicate that in countries with relatively low rice cultivation, the mapped areas generally exceed existing statistical data, shown as points below the  $y = x$  line in the fitting plot. In contrast, for countries with larger rice cultivation areas—such as the Democratic Republic of the Congo, Egypt, Guinea, Madagascar, Mali, and Tanzania—the mapped areas closely match existing statistics, with data points near the  $y = x$  line. While in Nigeria, the mapped rice  
355 cultivation area is significantly higher than existing statistics, represented by points far below the  $y = x$  line.

These discrepancies may be attributed to several factors. In developing countries in Africa, data collection and reporting systems are often incomplete and inconsistent, leading to major gaps in the accuracy of reported rice cultivation areas. The issue is further compounded by the dominance of smallholder farming systems, where individual farm sizes are smaller and scattered, making them even harder to track and report on accurately. This often results in underreporting or outdated figures  
360 in official statistics. Additionally, rice cultivation in these regions has undergone rapid changes in recent years, with some areas seeing significant increases in planting that aren't being fully captured by traditional reporting methods. Although multiple auxiliary datasets were integrated when constructing rice sample set for this study, the process still heavily relied on expert knowledge. This is particularly challenging in countries with limited rice cultivation, where rice fields are more difficult to identify, leading to sample errors that directly affect mapping accuracy. Moreover, the rice intensity distribution  
365 information used to estimate planting areas was published in 2017 and may not fully capture the present situation in 2023, contributing to discrepancies between the mapped data and reported cultivation areas.

### 3.4 Classification accuracy on validation set

The validation results for rice and non-rice classifications across 34 African countries provide a comprehensive insight into the model's performance. The table displays key metrics, including user accuracy (UA), producer accuracy (PA), F1 scores,  
370 and overall accuracy (OA). Analyzing these metrics offers an understanding of the spatial variations and classification challenges encountered across different regions.

#### Rice Classification Performance:

**User Accuracy (UA):** The UA for rice classification ranges from 65.26% in South Sudan to 97.51% in Rwanda. The lower values in countries like South Sudan and Niger highlight challenges in correctly identifying rice fields, possibly due to  
375 fragmented land use or small cultivation areas.



**Producer Accuracy (PA):** The PA for rice classification spans from 70.78% in South Sudan to 93.17% in Guinea. Higher PA values indicate the model's ability to correctly classify most rice areas, while lower values in regions like South Sudan suggest a tendency for rice areas to be misclassified as non-rice.

380 **F1 Score:** The F1 scores, combining precision and recall, vary from 67.91% in South Sudan to 94.54% in Guinea. While most countries maintain F1 scores above 80%, lower scores in regions like Angola and Niger highlight difficulties in balancing precision and recall.

#### **Non-Rice Classification Performance:**

**User Accuracy (UA):** The UA for non-rice ranges from 74.09% in South Sudan to 92.18% in Guinea, with most countries over 85%. High UA values across most countries indicate effective identification of non-rice areas.

385 **Producer Accuracy (PA):** The PA ranges from 68.92% in South Sudan to 96.55% in Rwanda. Most countries exceed 80%, underscoring consistent performance, though lower values in South Sudan indicate difficulties in distinguishing non-rice areas.

**F1 Score:** The F1 scores for non-rice range from 71.41% in South Sudan to 93.74% in Guinea. Countries with lower scores, such as Niger and Sudan, highlight specific regional challenges in sample set construction with very limited rice cultivation.

390 **Overall Accuracy (OA):**

The overall accuracy (OA) ranges from 69.76% in South Sudan to 94.17% in Guinea, with a mean of around 86.30%. Countries with extensive rice cultivation, such as Ghana and Senegal, show OAs above 90%, reflecting the model's robustness in regions with more homogeneous and concentrated rice production.

#### **Key Insights and Implications:**

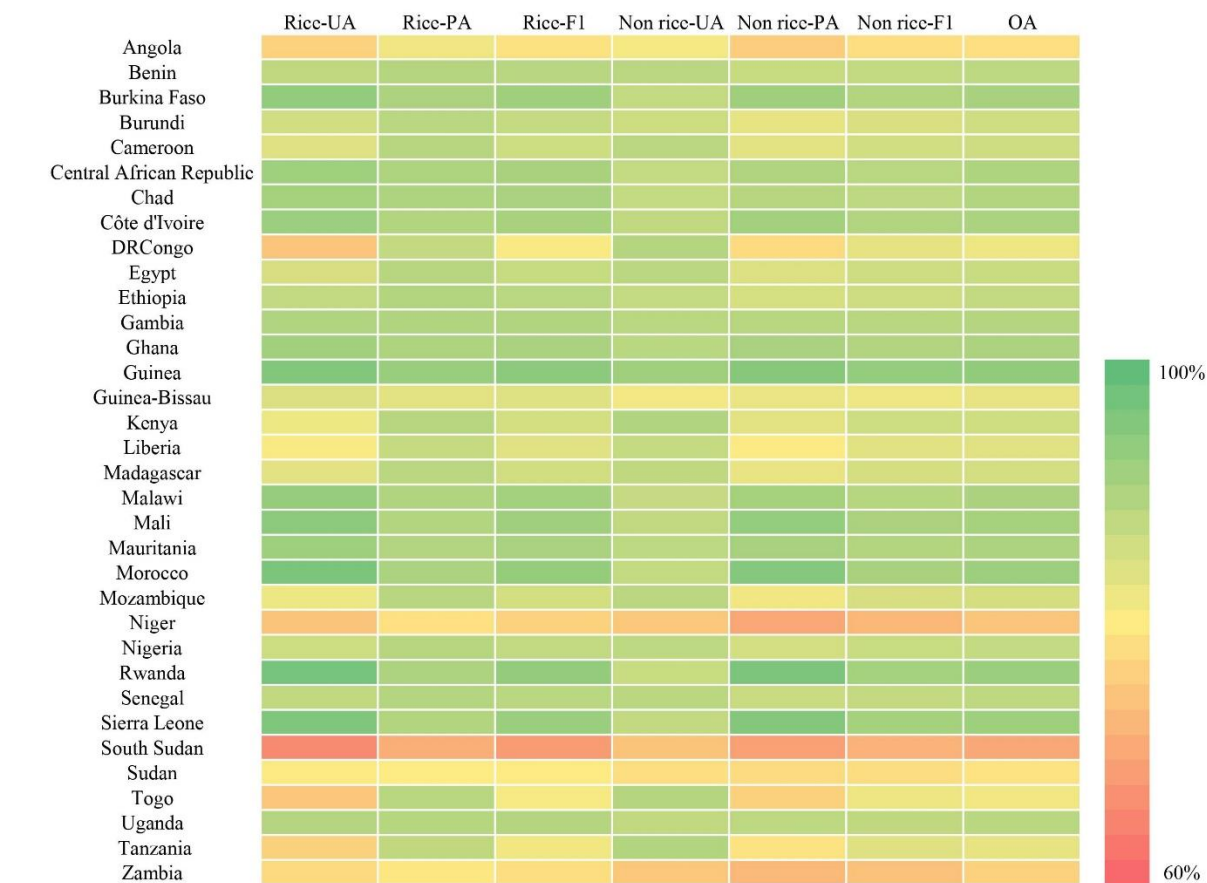
395 **Regional Variations:** The variations in accuracy metrics indicate that regional agricultural practices, land use complexity, and data quality play significant roles in model performance. Regions with small, fragmented rice fields or mixed cropping systems, such as South Sudan, Niger, and Angola, present classification challenges that lead to lower accuracy scores.

400 **Outliers and Challenges:** The box plot (Fig.12) analysis reveals stable and consistent performance across most countries, with median values clustering between 85% and 90%. However, outliers such as South Sudan, Angola, and Niger show lower accuracy scores, suggesting that additional refinement is needed for these regions.

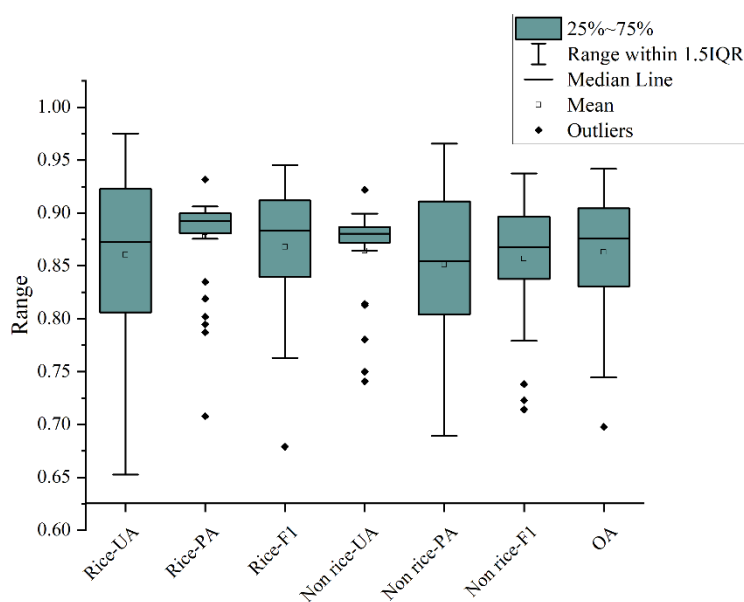
**Model Reliability:** The overall consistency in accuracy metrics across most countries highlights the robustness of the rice mapping methodology. Future improvements could focus on addressing the specific challenges faced in regions with complex agricultural landscapes or limited data availability.

405 The findings underscore the importance of tailored approaches when applying classification models across diverse African environments. Addressing regional discrepancies will be crucial in enhancing data accuracy and supporting better agricultural policy development across Africa.





(a)



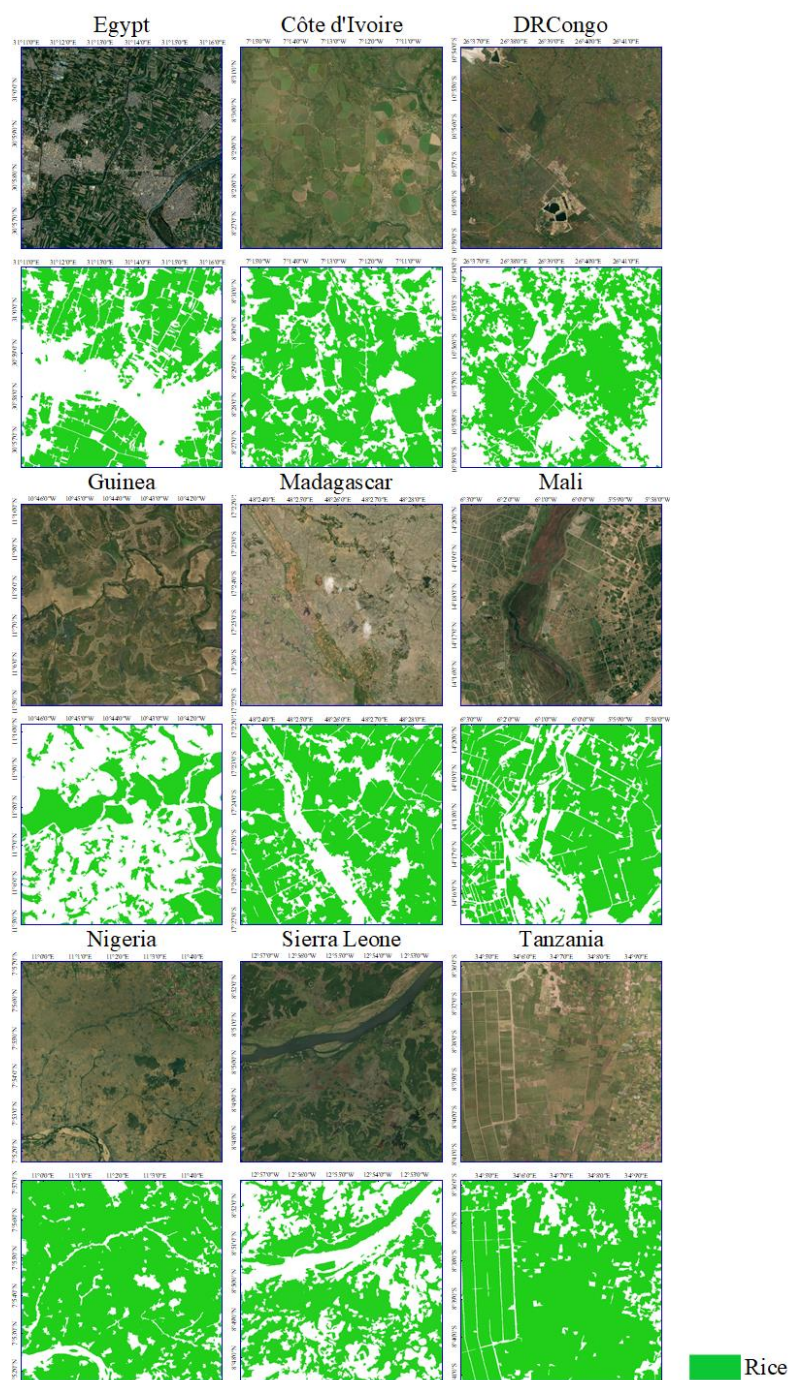
(b)



410 **Figure 13. Performance on validation set (a) heat map of validation accuracy across 34 African countries (b) corresponding box plot**

### 3.5 Comparison of rice mapping results with optical imagery

415 Fig. 14 illustrates the comparison between the rice mapping results and corresponding optical image for selected regions in nine major rice-producing countries in Africa (with rice field areas exceeding 500,000 hectares). The examples include both concentrated plantation zones and dispersed smallholder farming areas. The results show a strong alignment between the mapped outputs and the optical images. Additionally, due to the incorporation of the object-based segmentation step, the mapping results exhibit clear boundaries, minimal scattered noise, and fewer misclassifications.



420 **Figure 14.** Examples of rice mapping results and corresponding optical imagery for major rice-producing countries in Africa. For each country, the first row shows the optical imagery (from ©Google Earth), while the second row presents the rice mapping results, with green areas representing rice fields.



## 5 Discussion

### 5.1 Strengths and limitations

To produce large-scale, high-resolution rice distribution maps across Africa, this study proposed a method effectively combining Sentinel-1 SAR and Sentinel-2 optical imagery, addressing key challenges in sample collection and classification. 425 By leveraging time-series statistical features from Sentinel-1 VH data for initial fast coarse positioning of potential rice-planting areas and complementing this with visual interpretation using auxiliary datasets, the study efficiently generates reliable samples. During the classification phase, the approach integrates object-based segmentation results from Sentinel-2 optical time-series data with feature importance guided Random Forest classification results from Sentinel-1 SAR time-series data. This combination enhances the precision of rice paddy boundaries and reduces noise in heterogeneous 430 landscapes.

Despite these strengths, the study acknowledges limitations related to the SNIC algorithm, particularly in the calibration of key parameters—seed distance and neighbourhood size, which affects the size and definition of segmented objects. In this study, it was primarily achieved through a process of trial and visual inspection. While this method provided a practical solution within the context of this research, it lacks the precision and reproducibility necessary for wider application. Future 435 research should focus on developing more systematic approaches to parameter optimization. This could involve the use of automated tuning algorithms or machine learning techniques that adjust parameters dynamically based on the characteristics of the input data, thereby improving the accuracy, consistency, and scalability of the segmentation process.

Additionally, the study highlights regional variations in the importance of specific features for rice mapping across Africa. Despite these variations, temporal statistical features from SAR data—particularly VH, VV, and PRVI—consistently 440 demonstrated their utility in capturing the temporal dynamics of rice cultivation. By further exploring and experimenting with these temporal SAR features, future studies could refine rice detection models to be more sensitive to regional differences and temporal changes in Africa. This could involve integrating these features with additional data sources, such as optical imagery or other environmental variables, to create more robust and comprehensive mapping models. Such advancements would not only improve the accuracy of rice mapping in Africa but also contribute to better agricultural 445 monitoring and decision-making at a broader scale.

### 5.2 Progress and gaps in the National Rice Development Strategy (NRDS) of CARD countries towards 2030 targets

Comparing existing rice planting/harvesting statistics from African countries with the rice planting area results obtained in this study reveals that although rice cultivation in most African countries has fluctuated, there is still a slow upward trend. This aligns with the policy direction of promoting rice cultivation in these countries, though there remains a significant gap 450 to achieve the 2030 Rice Research and Innovation Strategy for Africa target. Among the countries assessed, 15 have achieved over 80% of the 2030 target, 5 have achieved 60–80%, 7 have achieved 40–60%, and 3 have achieved less than 40%. Of the 9 countries with completion rates below 60%, Tanzania, Senegal, Sierra Leone, and Burkina Faso currently



455 have substantial rice cultivation areas (greater than 200,000 hectares) but have set high targets. Ethiopia, Liberia, Sudan, Niger, and Kenya have smaller targets but still lag in their current rice cultivation. Countries should develop and adjust their rice cultivation strategies accordingly to achieve the “Transformation of Rice-based Agri-food Systems for Food and Nutrition Security in Africa” and enhance local food self-sufficiency, ultimately contributing to the SDG goal of zero hunger.

**Table 9. Current rice cultivation areas and 2030 targets for card countries (card 2022), sorted by completion percentage**

Num	Country	Result	Target/Ha	Ratio	Region
1	Angola	30375	11531	263%	Central
2	Central African Republic	70545	30350	232%	Central
3	Chad	501287	254580	197%	Central
4	Democratic Republic of the Congo	1523243	776000	196%	Central
5	Ghana	709060	372330	190%	Western
6	Burundi	102335	68244	150%	Eastern
7	Malawi	120866	82621	146%	Eastern
8	Uganda	368356	280000	132%	Eastern
9	Cameroon	403379	334764	120%	Central
10	Guinea-Bissau	178277	155046	115%	Western
11	Zambia	83916	80266	105%	Eastern
12	Rwanda	61969	60000	103%	Eastern
13	Togo	194153	193000	101%	Western
14	Benin	215851	242000	89%	Western
15	Gambia	206632	247009	84%	Western
16	Madagascar	1537131	2105690	73%	Eastern
17	Mozambique	415471	570272	73%	Eastern
18	Côte d'Ivoire	727320	1003580	72%	Western
19	Mali	914169	1283970	71%	Western
20	Guinea	1580359	2547881	62%	Western
21	Nigeria	4889668	8523687	57%	Western
22	United Republic of Tanzania	1160821	2200000	53%	Eastern
23	Senegal	384397	775053	50%	Western
24	Ethiopia	155157	327252	47%	Eastern
25	Burkina Faso	273063	627587	44%	Western
26	Sierra Leone	694314	1602103	43%	Western



27	Liberia	135214	326183	41%	Western
28	Sudan	52553	142856	37%	Northern
29	Niger	85573	252507	34%	Western
30	Kenya	59220	222000	27%	Eastern

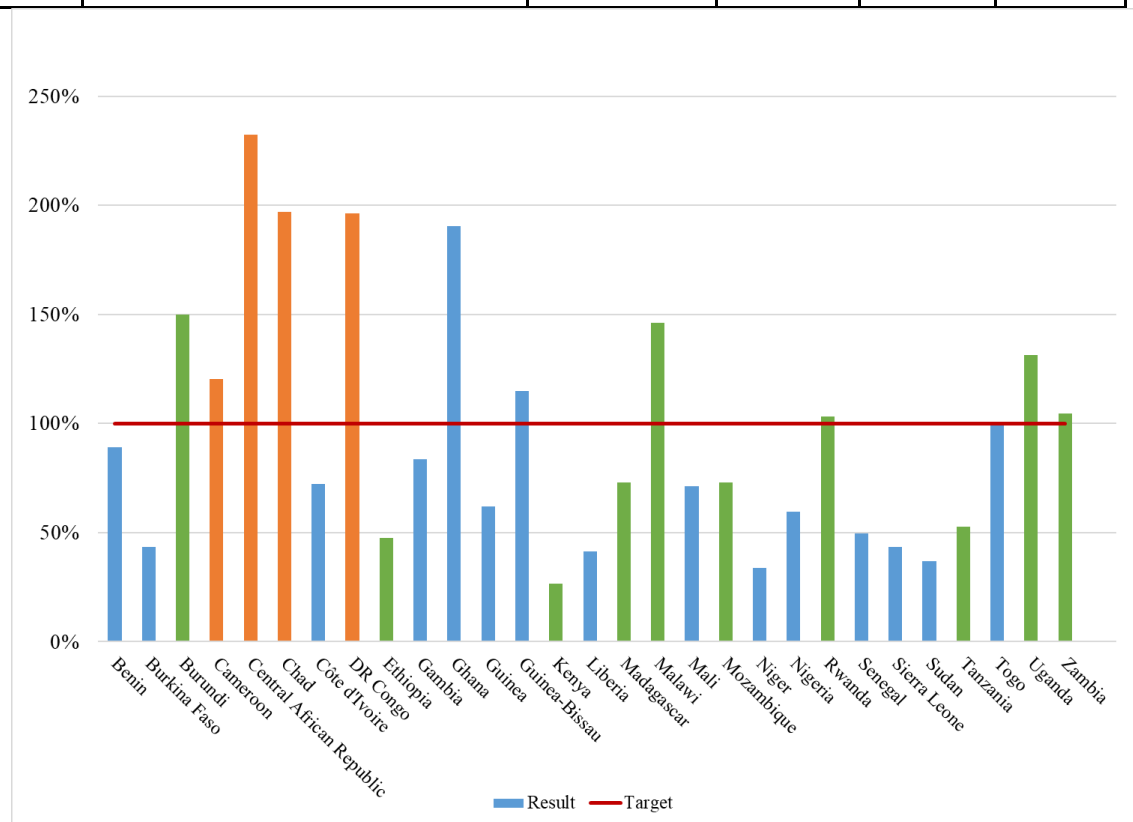


Figure 15. Comparison of current rice plating areas and 2030 targets for CARD countries

## 460 6 Data Availability

The 20m Africa Rice Distribution Map of 2023 can be accessed in the Zenodo data set from the following DOI: <https://doi.org/10.5281/zenodo.13729353> (Jiang, Zhang et al. 2024). The spatial reference system of the data set is EPSG:4326(WGS84).

## 7 Conclusion

465 This study employs temporal SAR data and optical imagery, combined with object-oriented segmentation, and feature importance guided random forest algorithms, to conduct rice extraction experiments in 34 African countries with annual rice



planting areas exceeding 5,000 hectares, achieving 20-meter resolution spatial distribution mapping of rice in Africa for 2023. The average classification accuracy on the validation set exceeded 85%, and the  $R^2$  values for linear fitting with existing statistical data all surpassed 0.9, demonstrating the effectiveness of the proposed mapping method.

470 This study marks the first time a high-resolution rice spatial distribution map has been generated for the entire African continent, offering significant advancements in monitoring rice cultivation patterns in the region. The map provides crucial data support for rice yield estimation, climate resilience assessments, and the development of targeted agricultural policies. Moreover, the insights derived from this research can aid in optimizing resource allocation, enhancing food security, and informing decision-making processes for stakeholders ranging from policymakers to local farmers across Africa.

475

**Author Contributions:** Conceptualization, methodology, software, J.J., M.S. and J.G; validation, formal analysis, J.J. and J.G.; investigation, J.J. and H.Z.; resources, data curation, L.X., Y.D. and Y.X.; writing—original draft preparation, J.J., and H.Z.; writing—review and editing, H.Z., L.X., J.G. and L.Z.; visualization, J.J., Y.D., Y.X.; supervision, project administration, H.Z., L.Z., and W.H.. All authors have read and agreed to the published version of the manuscript.

480 **Funding:** The research was supported by the International Research Centre of Big Data for Sustainable 455 Development Goals (CBAS) [grant numbers CBAS2023SDG001], and the National Key R&D Program of China [grant numbers 2023YFB390620X).

**Acknowledgments:** The authors acknowledge the support of data and computational power provided by the Google Earth Engine platform.

485 **Conflicts of Interest:** The authors declare no conflict of interest.

## References

- Achanta, R. and S. Susstrunk (2017). Superpixels and polygons using simple non-iterative clustering. Proceedings of the IEEE conference on computer vision and pattern recognition.
- 490 AfricaRice (2023). Africa Rice Center (AfricaRice). 2023. Transformation of Rice-based Agri-food Systems for Food and Nutrition Security in Africa: 2030 rice research and innovation strategy for Africa. Abidjan, Côte d'Ivoire: vi+58 pp.
- Ajala, A. and A. Gana (2015). "Analysis of challenges facing rice processing in Nigeria." Journal of food processing **2015**(1): 893673.
- Arouna, A., I. A. Fatognon, K. Saito and K. Futakuchi (2021). "Moving toward rice self-sufficiency in sub-Saharan Africa by 2030: Lessons learned from 10 years of the Coalition for African Rice Development." World Development Perspectives **21**: 100291.
- 495 Avcı, C., M. Budak, N. Yağmur and F. Balçık (2023). "Comparison between random forest and support vector machine algorithms for LULC classification." International Journal of Engineering and Geosciences **8**(1): 1-10.
- Balasubramanian, V., M. Sie, R. J. Hijmans and K. Otsuka (2007). Increasing Rice Production in Sub-Saharan Africa: Challenges and Opportunities. Advances in Agronomy. D. L. Sparks, Academic Press. **94**: 55-133.
- 500 Barro, M., A. I. Kassankogno, I. Wonni, D. Sereme, I. Somda, H. K. Kabore, G. Bena, C. Brugidou, D. Tharreau and C. Tollenaere (2021). "Spatiotemporal Survey of Multiple Rice Diseases in Irrigated Areas Compared to Rainfed Lowlands in the Western Burkina Faso." Plant Dis **105**(12): 3889-3899.
- Bhogapurapu, N., S. Dey, D. Mandal, A. Bhattacharya, L. Karthikeyan, H. McNairn and Y. Rao (2022). "Soil moisture retrieval over croplands using dual-pol L-band GRD SAR data." Remote Sensing of Environment **271**: 112900.



- 505 CARD. (2022). "COALITION for African Rice Development: COUNTRIES." from <https://riceforafrica.net/>.  
Chang, J. G., M. Shoshany and Y. Oh (2018). "Polarimetric radar vegetation index for biomass estimation in desert fringe ecosystems." *IEEE Transactions on Geoscience and Remote Sensing* **56**(12): 7102-7108.  
Charbonneau, F., M. Trudel and R. Fernandes (2005). *Use of Dual Polarization and Multi-Incidence SAR for soil permeability mapping*. Proceedings of the 2005 advanced synthetic aperture radar (ASAR) workshop, St-Hubert, QC, Canada.
- 510 Chhabra, A., C. Rüdiger, M. Yebra, T. Jagdhuber and J. Hilton (2022). "RADAR-Vegetation Structural Perpendicular Index (R-VSPI) for the Quantification of Wildfire Impact and Post-Fire Vegetation Recovery." *Remote Sensing* **14**(13): 3132.  
FAO. (2022). "FAOSTAT: Crops and livestock products." from <https://www.fao.org/faostat/en/#data/QCL>.  
FAO (2023). "World Food and Agriculture – Statistical Yearbook 2023."
- 515 FEWSNET. (2018). "Livelihoods Zone Map and Descriptions for South Sudan."  
Field, C. B. and V. R. Barros (2014). *Climate change 2014–Impacts, adaptation and vulnerability: Regional aspects*, Cambridge University Press.  
Frolking, S., D. Wisser, D. Grogan, A. Proussevitch and S. Glidden (2020). GAEZ+\_2015 Crop Harvest Area, Harvard Dataverse.
- 520 Ginting, F. I., R. Rudiyanto, Fatchurahman, R. Mohd Shah, N. Che Soh, S. G. E. Giap, D. Fiantis, B. I. Setiawan, S. Schiller and A. Davitt (2024). "SEA-Rice-C110: High-resolution Mapping of Rice Cropping Intensity and Harvested Area Across Southeast Asia using the Integration of Sentinel-1 and Sentinel-2 Data." *Earth System Science Data Discussions* **2024**: 1-49.  
Gorelick, N., M. Hancher, M. Dixon, S. Ilyushchenko, D. Thau and R. Moore (2017). "Google Earth Engine: Planetary-scale geospatial analysis for everyone." *Remote sensing of Environment* **202**: 18-27.
- 525 Guan, X., C. Huang, G. Liu, X. Meng and Q. Liu (2016). "Mapping Rice Cropping Systems in Vietnam Using an NDVI-Based Time-Series Similarity Measurement Based on DTW Distance." *Remote Sensing* **8**(1): 19.  
Guo, Y., X. Jia, D. Paull and J. A. Benediktsson (2019). "Nomination-favoured opinion pool for optical-SAR-synergistic rice mapping in face of weakened flooding signals." *ISPRS Journal of Photogrammetry and Remote Sensing* **155**: 187-205.  
Han, J., Z. Zhang, Y. Luo, J. Cao, L. Zhang, F. Cheng, H. Zhuang, J. Zhang and F. Tao (2021). "NESEA-Rice10: high-resolution annual paddy rice maps for Northeast and Southeast Asia from 2017 to 2019." *Earth System Science Data* **13**(12): 5969-5986.
- 530 Hussain, S., J. Huang, J. Huang, S. Ahmad, S. Nanda, S. Anwar, A. Shakoor, C. Zhu, L. Zhu and X. Cao (2020). "Rice production under climate change: adaptations and mitigating strategies." *Environment, climate, plant and vegetation growth*: 659-686.
- 535 International Food Policy Research, I. (2020). Spatially-Disaggregated Crop Production Statistics Data in Africa South of the Sahara for 2017. I. International Food Policy Research, Harvard Dataverse.  
Jiang, J., H. Zhang, J. Ge, L. Zuo, L. Xu, M. Song, Y. Ding, Y. Xie and W. Huang (2024). 20m Africa rice distribution map in 2023 [dataset], <https://doi.org/10.5281/zenodo.13729353>.  
Kuenzer, C. and K. Knauer (2013). "Remote sensing of rice crop areas." *International Journal of Remote Sensing* **34**(6): 2101-2139.
- 540 Laborte, A. G., M. A. Gutierrez, J. G. Balanza, K. Saito, S. J. Zwart, M. Boschetti, M. V. R. Murty, L. Villano, J. K. Aunario, R. Reinke, J. Koo, R. J. Hijmans and A. Nelson (2017). "RiceAtlas, a spatial database of global rice calendars and production." *Scientific Data* **4**(1).  
Li, J. and S. Wang (2018). "Using SAR-Derived Vegetation Descriptors in a Water Cloud Model to Improve Soil Moisture Retrieval." *Remote Sensing* **10**(9): 1370.
- 545 Liu, X., H. Zhai, Y. Shen, B. Lou, C. Jiang, T. Li, S. B. Hussain and G. Shen (2020). "Large-scale crop mapping from multisource remote sensing images in google earth engine." *IEEE Journal of Selected Topics in Applied Earth Observations and Remote Sensing* **13**: 414-427.
- 550 Loko, Y. L. E., C. D. S. J. Gbemavo, G. Djedatin, E.-E. Ewedje, A. Orobiyi, J. Toffa, C. Tchakpa, P. Sedah and F. Sabot (2022). "Characterization of rice farming systems, production constraints and determinants of adoption of improved varieties by smallholder farmers of the Republic of Benin." *Scientific Reports* **12**(1): 3959.  
Luo, K., L. Lu, Y. Xie, F. Chen, F. Yin and Q. Li (2023). "Crop type mapping in the central part of the North China Plain using Sentinel-2 time series and machine learning." *Computers and Electronics in Agriculture* **205**: 107577.  
Mathieu, R. (2022). "Mapping of Rice Areas in Egypt using SAR Imagery."





- 555 Ogisi, O. D. and T. Begho (2023). "Adoption of climate-smart agricultural practices in sub-Saharan Africa: A review of the progress, barriers, gender differences and recommendations." *Farming System* **1**(2): 100019.
- Qiu, B., W. Li, Z. Tang, C. Chen and W. Qi (2015). "Mapping paddy rice areas based on vegetation phenology and surface moisture conditions." *Ecological Indicators* **56**: 79-86.
- 560 Saad El Imanni, H., A. El Harti, M. Hssaisoune, A. Velastegui-Montoya, A. Elbouzidi, M. Addi, L. El Iysaouy and J. El Hachimi (2022). "Rapid and automated approach for early crop mapping using Sentinel-1 and Sentinel-2 on Google earth engine; a case of a highly heterogeneous and fragmented agricultural region." *Journal of Imaging* **8**(12): 316.
- Seck, P. A., A. Diagne, S. Mohanty and M. C. Wopereis (2012). "Crops that feed the world 7: Rice." *Food security* **4**: 7-24.
- Shen, R., B. Pan, Q. Peng, J. Dong, X. Chen, X. Zhang, T. Ye, J. Huang and W. Yuan (2023). "High-resolution distribution maps of single-season rice in China from 2017 to 2022." *Earth System Science Data Discussions* **2023**: 1-27.
- 565 Singh, R. K., J. Rizvi, M. D. Behera and C. Biradar (2021). "Automated crop type mapping using time-weighted dynamic time warping-A basis to derive inputs for enhanced food and Nutritional Security." *Current Research in Environmental Sustainability* **3**: 100032.
- Sun, C., H. Zhang, L. Xu, J. Ge, J. Jiang, M. Song and C. Wang (2024). "Rice yield prediction using radar vegetation indices from Sentinel-1 data and multiscale one-dimensional convolutional long-and short-term memory network model." *Journal of Applied Remote Sensing* **18**(2): 024505-024505.
- 570 Sun, C., H. Zhang, L. Xu, J. Ge, J. Jiang, L. Zuo and C. Wang (2023). "Twenty-meter annual paddy rice area map for mainland Southeast Asia using Sentinel-1 synthetic-aperture-radar data." *Earth System Science Data* **15**(4): 1501-1520.
- Tang, F. H., T. H. Nguyen, G. Conchedda, L. Casse, F. N. Tubiello and F. Maggi (2023). "CROPGRIDS: A global georeferenced dataset of 173 crops circa 2020." *Earth System Science Data Discussions* **2023**: 1-22.
- 575 Tassi, A. and M. Vizzari (2020). "Object-oriented lulc classification in google earth engine combining snic, glcm, and machine learning algorithms." *Remote Sensing* **12**(22): 3776.
- Tian, G., H. Li, X. Feng, Q. Jiang, N. Li, Z. Guo, J. Zhao and H. Yang (2024). "An automatic method for rice mapping in Taishan, China using Sentinel-1A Time-series images." *Remote Sensing Letters* **15**(1): 99-109.
- USDA. (2023). "Foreign Agricultural Service." from <https://ipad.fas.usda.gov/countrysummary>.
- 580 Waleed, M., M. Mubeen, A. Ahmad, M. Habib-ur-Rahman, A. Amin, H. U. Farid, S. Hussain, M. Ali, S. A. Qaisrani and W. Nasim (2022). "Evaluating the efficiency of coarser to finer resolution multispectral satellites in mapping paddy rice fields using GEE implementation." *Scientific Reports* **12**(1): 13210.
- Wang, G., D. Meng, R. Chen, G. Yang, L. Wang, H. Jin, X. Ge and H. Feng (2024). "Automatic Rice Early-Season Mapping Based on Simple Non-Iterative Clustering and Multi-Source Remote Sensing Images." *Remote Sensing* **16**(2): 277.
- 585 Wang, Y., S. Zang and Y. Tian (2020). "Mapping paddy rice with the random forest algorithm using MODIS and SMAP time series." *Chaos, Solitons & Fractals* **140**: 110116.
- Wei, J., Y. Cui, W. Luo and Y. Luo (2022). "Mapping paddy rice distribution and cropping intensity in China from 2014 to 2019 with landsat images, effective flood signals, and google earth engine." *Remote Sensing* **14**(3): 759.
- 590 Wu, H., J. Zhang, Z. Zhang, J. Han, J. Cao, L. Zhang, Y. Luo, Q. Mei, J. Xu and F. Tao (2022). "AsiaRiceYield4km: seasonal rice yield in Asia from 1995 to 2015." *Earth System Science Data Discussions* **2022**: 1-30.
- You, N., J. Dong, J. Huang, G. Du, G. Zhang, Y. He, T. Yang, Y. Di and X. Xiao (2021). "The 10-m crop type maps in Northeast China during 2017-2019." *Sci Data* **8**(1): 41.
- You, N., J. Dong, J. Huang, G. Du, G. Zhang, Y. He, T. Yang, Y. Di and X. Xiao (2021). "The 10-m crop type maps in Northeast China during 2017-2019." *Scientific data* **8**(1): 41.
- 595 Yu, Q., L. You, U. Wood-Sichra, Y. Ru, A. K. Joglekar, S. Fritz, W. Xiong, M. Lu, W. Wu and P. Yang (2020). "A cultivated planet in 2010-Part 2: The global gridded agricultural-production maps." *Earth System Science Data* **12**(4): 3545-3572.
- Yuan, S., K. Saito, P. A. J. van Oort, M. K. van Ittersum, S. Peng and P. Grassini (2024). "Intensifying rice production to reduce imports and land conversion in Africa." *Nature Communications* **15**(1): 835.
- 600 Zhan, P., W. Zhu and N. Li (2021). "An automated rice mapping method based on flooding signals in synthetic aperture radar time series." *Remote Sensing of Environment* **252**: 112112.
- Zhang, W., H. Liu, W. Wu, L. Zhan and J. Wei (2020). "Mapping rice paddy based on machine learning with Sentinel-2 multi-temporal data: Model comparison and transferability." *Remote Sensing* **12**(10): 1620.



- 605 Zhang, X., R. Shen, X. Zhu, B. Pan, Y. Fu, Y. Zheng, X. Chen, Q. Peng and W. Yuan (2023). "Sample-free automated mapping of double-season rice in China using Sentinel-1 SAR imagery." *Frontiers in Environmental Science* **11**.
- Zhu, A.-X., F.-H. Zhao, H.-B. Pan and J.-Z. Liu (2021). "Mapping rice paddy distribution using remote sensing by coupling deep learning with phenological characteristics." *Remote sensing* **13**(7): 1360.
- 610 Zoungrana, L. E., M. Barbouchi, W. Toukabri, M. O. Babasy, N. B. Khatra, M. Annabi and H. Bahri (2024). "Sentinel SAR-optical fusion for improving in-season wheat crop mapping at a large scale using machine learning and the Google Earth engine platform." *Applied Geomatics* **16**(1): 147-160.